European Journal of Immunology

WILEY-VCH

European Journal of Immunology Basic • Clinical • Translational

RESEARCH ARTICLE OPEN ACCESS

Molecular Immunology and Signaling

SYK Signalling in NLRP3 Inflammasome-Mediated Response of Murine Microglia Activated by Immune Complexes Formed of Viral Proteins and Specific IgG

Kristina Mašalaitė | Milda Norkienė | Aurelija Žvirblienė | Asta Lučiūnaitė

Institute of Biotechnology, Life Sciences Center, Vilnius University, Vilnius, Lithuania

Correspondence: Kristina Mašalaitė (kristina.masalaite@gmc.vu.lt)

Received: 23 October 2025 | **Revised:** 13 April 2026 | **Accepted:** 22 April 2026

Keywords: antigen presentation | immune complexes | NLRP3 | SYK

ABSTRACT

Viral infections might trigger systemic inflammatory responses characterised by inflammasome activation and cytokine release, driven by immune complex (IC) formation, but the precise mechanism remains unknown. The NLRP3 inflammasome is a vital component of innate immunity that plays a significant role in inflammatory responses. The involvement of the non-receptor spleen tyrosine kinase (SYK) in the activation of the NLRP3 inflammasome has been demonstrated. SYK plays a critical role in signal transduction pathways of immunoreceptors and regulates NLRP3 inflammasome activation. Our previous study showed that viral antigens and their IC with specific antibodies trigger NLRP3 inflammasome activation in macrophages. Therefore, we studied the role of SYK in IC-induced NLRP3 inflammasome activation pathway using primary mouse microglia as a macrophage model. The inflammasome activation was analysed by measuring cytokine secretion, ASC speck formation, and NLRP3 expression. To link SYK activation to NLRP3 inflammasome activation and other macrophage functional properties, we employed a specific SYK inhibitor, R406. We demonstrated SYK involvement in NLRP3 inflammasome activation by viral IC and in SYK-dependent antigen presentation in microglia after IC phagocytosis. Our findings also revealed lipid raft clustering upstream of SYK activation. These results may explain the mechanisms behind severe inflammation caused by viral IC.

1 | Introduction

The first line of host defence is innate immune cells, and the main part of them are monocytes/macrophages. Macrophages are key tissue sentinel cells present across various organs at high density, playing a vital role in removing pathogens, initiating immune response, regenerating tissues, and maintaining homeostasis [1]. Macrophages are equipped with various tools to perform their functions, for instance, a variety of pattern-recognition receptors (PRR), which promote phagocytosis, antigen presentation, and release of inflammatory mediators. One specific cytoplasmic PRR that can form an inflammasome is the NLR family pyrin domain-containing (NLRP3) receptor, which might be triggered not only by a limited number of pathogenic molecules, but also by environmental irritants and metabolic products [2]. When the NLRP3 receptor responds to a stimulus, such as PAMPs or DAMPs, it oligomerizes to form a large multimeric immune complex, the NLRP3 inflammasome [3]. NLRP3 inflammasome consists of three major components—the NLRP3 receptor, apoptosis-associated speck-like protein containing a caspase-recruitment domain (ASC), and autoproteolytically activating caspase-1 [4]. The activity of multiple signalling receptors tightly controls the

Abbreviations: IC, immune complexes; mAb, monoclonal antibody; SYK, spleen tyrosine kinase; VLP, virus-like particle.

expression of NLRP3 itself, as the activation of nuclear factor (NF)-κB is necessary for NLRP3 inflammasome formation [5]. The NLRP3 inflammasome activation results in the secretion of inflammatory cytokines IL-1β and IL-18 and inflammatory cell death, pyroptosis [6]. Although the NLRP3 inflammasome is essential in host innate immune defence against bacteria, fungi, and viruses, its activation has been linked to several inflammatory disorders, including Alzheimer's disease, autoinflammatory disorders, and severe viral hyperinflammation [6–8].

In the pathway of pathogen-induced NLRP3 activation, a non-receptor tyrosine kinase—spleen tyrosine kinase (SYK) is involved [9]. SYK is expressed in haematopoietic cells, particularly in monocytes and macrophages. It was reported that SYK participates in the signalling via PRRs, such as C-type lectin [10]. In pathogen-related inflammation induced by parasites or fungi, SYK transmits multiple crucial signals and regulates inflammatory cytokine secretion, cell migration, pathogen clearance, and even NLRP3 activation through ASC phosphorylation [11]. Nevertheless, SYK is most frequently identified as a signal transduction molecule in signalling pathways of immunoreceptors such as T cell receptor (TCR), B cell receptor (BCR), or activating Fcγ receptors (FcγRs), which are associated with cytoplasmic domains containing immunoreceptor tyrosine-based activation motifs (ITAMs) that are rapidly phosphorylated following receptor engagement, leading to the recruitment and activation of SYK [9]. Four different classes of FcγRs, known as FcγRI, FcγRIIB, FcγRIII, and FcγRIV, and four immunoglobulin G (IgG) subclasses (IgG1, IgG2a, IgG2b, and IgG3), which bind with varying affinity and specificity to different FcγRs, have been recognised in mice [12]. FcγRI can engage monomeric IgG with high affinity, while other FcγRs exhibit low affinity for IgGs and can only interact with multimeric IgG exposed on IC or opsonised cells, generated during an infectious challenge [13]. The Fc regions of antibodies on IgG-coated targets, such as opsonised pathogens or IC, cross-link with FcγRs on immune cells, leading to the target's internalisation with associated activation of downstream signalling cascades [14]. In detail, recognition of multiple IgGs and cross-linking of FcγRs cause receptor clustering and aggregation, leading to the ITAM domain's phosphorylation by SRC family kinases, then the recruitment and activation of SYK kinase [13]. Internalisation by activating FcγRs favours a degradative route for antigen processing and presentation that leads to T cell activation. Antigen uptake through distinct FcγRs may define its processing pathway and the repertoire of antigen epitopes presented [15]. Although FcγR signalling and pathogen opsonisation, usually, are related to pathogen uptake, degradation, and local inflammation, it was reported that IgG auto-antibodies and the uptake of antibody-opsonised virus by FcγR cause severe SARS-CoV-2 infection and systemic inflammation, which could be blocked by SYK inhibition [16]. Moreover, in cases of severe SARS-CoV-2 infection, activation of the NLRP3 inflammasome was also suggested as one of the key mediators of inflammation [17, 18]. Although there is a lack of research that links FcγRs signalling with NLRP3 inflammasome, these findings suggest that SYK might be involved in NLRP3 activation by FcγRs ligation with IC formed by viral antigens. However, detailed SYK-dependent signalling pathways are unknown.

We have shown earlier that, depending on structural properties and features of antigen–antibody interaction, formation of IC can significantly enhance the inflammatory response induced by viral antigens and activate NLRP3 inflammasome in macrophages [19]. In this study, we employed virus-like particles (VLPs) derived from the major capsid protein VP1 of human polyomavirus as a model viral antigen. VLPs mimic the native structure of the virus. Here, we aimed to elaborate on the latter research and analyse SYK activation by VLPs and their IC with VLP-specific IgG, focusing on the inflammasome activation and antigen presentation in macrophages. We used recombinant VLPs assembled from the VP1 protein of human polyomavirus and a collection of murine VLP-specific monoclonal antibodies (mAbs) of different subtypes.

2 | Materials and Methods

2.1 | Materials

Dulbecco's modified Eagle's medium (DMEM; 31966047), Dulbecco's Phosphate Buffered Saline (DPBS; #14190250), fetal bovine serum (FBS; #10500-064), penicillin/streptomycin (P/S; #15140122) were obtained from Gibco, Thermo Fischer Scientific. Cell culture plates: Cell Culture Flasks, 250 mL, 75cm^2 Cellstar (#658175) were from Greiner, Thermo Fischer Scientific; 3cm^2 cell culture dish plate TPP Multi-well tissue culture plates and dishes (#92006, #92012, #92024, #92048, #93040) were from TPP Techno Plastic Products AG; 8-well μ-slides (#80826, #80841, #80827) were from Ibidi. SYK kinase inhibitor R406 (#inh-r406), NLRP3 inhibitor MCC950 (#inh-mcc), and Zymosan (#tlrl-zyn) were from Invivogen. Cytochalasin D (#C8273) from Sigma-Aldrich. Hoechst 33342 Fluorescent Nucleic Acid Stain (Hoechst, #260-639) and Propidium Iodide Stain (PI, #260-638) from ImmunoChemistry Technologies. Dimethylsulfoxide (DMSO; #A3672) was from PanReac AppliChem and the ITW Reagents. Halt Protease/Phosphatase Inhibitor Cocktail (100X, #78400) and chemiluminescent substrate SuperSignal West Pico PLUS (#34577) were from Thermo Fisher Scientific. Cell Lysis Buffer (#9803) was from Cell Signaling Technology. "NeA-Blue" 3,3′,5,5′-Tetramethylbenzidine (TMB) substrate (#01016-1-1000) was from Clinical Science Products. Bovine Serum Albumin (BSA, #P06-1391000) from PAN-Biotech. RC syringe filter (cat#PA49.1), Tween-20 (#9127.1), and sulphuric acid (#X873.1) were from CarlRoth. Mouse IL-1 ß Uncoated ELISA Kit (#88-7013-77), TNF alpha Uncoated ELISA Kit (#88-7324-76), pHrodo iFL Green STP ester amine-reactive dye (#P36013), and pHrodo iFL Red STP ester amine-reactive dye (#P36010) were from Invitrogen, Thermo Fischer Scientific.

2.2 | Cell Culture

Primary mouse microglia culture was prepared as mentioned before [19]. For macrophage culture preparation, C57BL/6 newborn mice (1–3 days old) were received from Life Sciences Center of Vilnius University (Vilnius, Lithuania), which has State Food and Veterinary Service permissions to breed and use experimental animals for scientific purposes (Veterinary certificate No. LT 59–13-001 and Permission No. LT 61-13-004). Mature microglia were collected by shaking them off the glial cell monolayer. The cells were seeded at a 1×10^5/cm^2 density with 50% of old medium (conditioned medium in which microglia grew), and 50% new

DMEM medium complemented with 10% FBS, 1% P/S. Microglia collection was repeated up to three more times, 2–3 days apart. The next day, seeded microglia were washed and treated with serum-free DMEM complemented with 1% P/S. MAbs, VLPs, and their IC were used for microglia treatment. For IC formation, 20 μg/mL (500 mM) of VLPs and 7.5 μg/mL (50 mM) of VLP-specific IgG were mixed in serum-free medium and incubated for 30 min at 37°C. We also used 1 μM working concentration of SYK kinase inhibitor R406 or NLRP3 inhibitor MCC950 1 h before microglia treatment. Cytochalasin D was used for phagocytosis analysis and was added 30 min before treatment. After 24 h or 3 h incubation with treatment factors, cell supernatants were collected for ELISA or LDH analysis, and microglia were either lysed for Western blot or stained for Flow cytometry analysis and fluorescent microscopy.

2.3 | Preparation of VLPs and Antibodies

For microglia treatment, we used recombinant VLPs derived from Washington University human polyomavirus (WUPyV) composed of 360 monomers of WUPyV recombinant major capsid protein VP1 (MW 40 kDa) and a collection of in-house-generated murine monoclonal antibodies (mAbs) against WUPyV VLPs. The VLPs were produced in the *S. cerevisiae* yeast expression system and purified by CsCl density gradient centrifugation as described previously [20]. The mAbs—#11D2 clone of IgG1 isotype, #12F8, #4E12 clones of IgG2a isotype, and #5H10 clone of IgG2b isotype, were purified from hybridoma growth medium as described previously and stored in DPBS solution [19]. Cell culture-grade water was used in each purification step. Negative VLPs control—disassembled VLPs (VP1 pentamers) were also prepared. Non-denaturing purification buffers lacking L-arginine [21] were used to produce disassembled VLPs (VP1 pentamers). The methodology was identical to that described by Norkiene et al. [20] for VLP generation, except that L-arginine was omitted from all buffers. The formation of VP1 pentamers, rather than higher-order VLP capsomers, was confirmed by electron microscopy (Figure S1B).

2.4 | Staining of VLPs and mAbs With pHrodo Amine-Reactive Dyes

Phagocytosis analysis was performed with VLPs stained with the amine-reactive pH-sensitive pHrodo iFL Green STP ester, amine-reactive dye, and mAbs stained with pHrodo iFL Red STP ester, amine-reactive dye. Labeling was performed according to the manufacturer's protocol. Briefly, pHrodo Green dye was mixed with VLPs at a 5X molar excess. After 1 h incubation in the dark, the conjugate was dialysed overnight in DPBS. A 600-fold conjugate volume of DPBS was used for dialysis. After dialysis, the conjugate was diluted in glycerol 1:1 and stored at −20°C.

2.5 | Cytokine Detection

The concentrations of cytokines (IL-1β and TNF-α) in cell culture supernatants were measured using Uncoated ELISA kits (Mouse TNF alpha Uncoated ELISA kit and Mouse IL-1 beta Uncoated ELISA kit). The assays were based on the sandwich ELISA, and all procedures were performed according to the manufacturer's protocol. Supernatants were diluted up to 1:20. In the last step, 1 M H_2SO_4 solution was added to neutralize the HRP and substrate reaction. The plates were read at 450 nm wavelength with a Multiskan Go microplate spectrophotometer.

2.6 | Western Blot

Western blot assay was applied to determine SYK, phosphorylated SYK (pSYK), and NLRP3 protein expression. Sample preparation and Western blotting were done as described previously [19]. After protein transfer, membranes were incubated with primary antibodies against NLRP3 or pSYK diluted 1:1000 in TBST with 1% BSA overnight at 4°C. Primary antibodies used: anti-NLRP3 (D4D8T) rabbit mAb (#15101), Phospho-Syk (Tyr525/526) (C87C1) Rabbit mAb (#2710), and Phospho-Zap-70 (Tyr319)/Syk (Tyr352) rabbit pAb (#2701) from Cell Signaling Technology. Then, secondary antibodies—goat Anti-rabbit IgG, HRP-linked #7074 (Cell Signaling Technology) diluted 1:3000 in TBST with 1% BSA were applied for 1 h at room temperature. The HRP enzymatic reaction was developed using SuperSignal West Pico PLUS chemiluminescent substrate. For loading control detection, primary anti-β-Actin (BA3R) mouse mAb (#MA5-15739) from Invitrogen, Thermo Fisher Scientific, and Goat anti-Mouse IgG (H+L)-HRP conjugate (#1721011) from Bio-Rad, diluted at a ratio of 1:1000 and 1:4000, respectively, in TBST with 1% BSA. The HRP reaction was developed as mentioned above. Chemiluminescent detection was performed with the Azure 280 imaging system. The ImageJ program was used to analyse Western blot data quantitatively.

2.7 | Immunocytochemistry for ASC Speck, pSYK, and Lipid Raft Detection

Microglia preparation for immunocytochemical staining was the same as described previously [19]. After blocking, the cells were stained with rabbit anti-ASC polyclonal antibodies (#AL177, Adipogen) or pSYK (Tyr525/526) (C87C1) Rabbit mAb (#2710) ON at 4°C. The next day, cells were washed with DPBS and incubated for 1 h with goat anti-rabbit IgG antibodies conjugated with Alexa Fluor 488 (# A11029, Invitrogen). For lipid raft staining before fixation, cells were incubated for 10 min on ice and stained with Cholera Toxin Subunit B (Recombinant) Alexa Fluor 594 Conjugate (#C34777, Invitrogen), 1:500 diluted in PBS for 30 min on ice in the dark. Then, cells were washed with DPBS, fixed with 4% PFA, blocked with 2% BSA in DPBS, and stained with Goat anti-Mouse IgG (H+L) Secondary Antibody, Alexa Fluor 488 (#A11029, Invitrogen) diluted 1:1000 in DPBS for an hour to detect colocalisation of lipid rafts and immune complexes on the cell surface. Nuclei were stained with Hoechst 33342 1 μg/mL (H3570, Invitrogen) for 20 min at room temperature. After staining, the cells were washed twice and analysed under a fluorescent microscope. For ASC speck analysis, EVOS FL Auto microscope, and for the lipid raft colocalisation or pSYK analysis, LEICA TCS SP8 confocal and Nikon Eclipse Ti-2E wide-field microscopes were used.

2.8 | Flow Cytometry

After treatment, cells were washed with DPBS once and incubated with Versen (Gibco) for 10 min at 37°C. Then, the cells were scraped, collected into a V-shaped 96-well plate, and centrifuged at 400 *g* for 10 min. After centrifugation, cells were washed and blocked with TruStain FcX anti-mouse CD16/32 antibody (#101319, BioLegend) for 15 min. Then, cells were stained with Anti-MHC Class II (I-A/I-E) (M5/114.15.2) Rat mAb redFluor 710 Conjugate (#29097S, Cell Signaling) 1:50, Anti-CD86-PE, clone GL1 (#A16385, Life Technologies) 1:100, and Anti-CD11b- Brilliant Violet 786 (BV786), clone M1/70 (#417-0112-82, Life Technologies) 1:50 for 2 h on ice. After staining, cells were washed, centrifuged, resuspended, stained with 7AAD viability staining solution (#00-6993-50, Life Technologies) for 5 min, and analysed with the BD Symphony A1 flow cytometer. Data analysis and visualisation were done with FlowJo v10.10.0 software.

2.9 | Statistical Analysis

Statistical analysis was performed with GraphPad Prism 10.1.0 software (GraphPad Software, Inc., La Jolla, CA). The data are presented as box plots (showing minimum, first quartile, median, third quartile, and maximum) or bar graphs (mean and SD) with individual data points of at least four independent experiments (*N*) indicating the number of independent cell culture preparations. A normality test was conducted to test whether the values came from a Gaussian distribution. Statistical comparisons of treatments were performed with one-way ANOVA in conjunction with Tukey's multiple comparison test or Student's *t*-test. A Kruskal–Wallis test with Dunn's post hoc test was used for non-parametric data. Differences with p values less than 0.05 were considered statistically significant: $^{*}p < 0.05$, $^{**}p < 0.01$, $^{***}p < 0.001$, $^{****}p < 0.0001$.

3 | Results

3.1 | SYK-Dependent NLRP3 Activation by Viral IC in Primary Mouse Microglia

To unravel the SYK role in macrophage activation, we first analysed SYK activation by IC composed of VLPs and their specific mAbs. We chose primary mouse microglia as a model for innate immune responses because microglia responses are analogous to tissue macrophages, one of the first responders to any pathogen [22]. Immunocytochemical staining of pSYK and fluorescent microscopy were applied to determine SYK activation. From microscopy data, it was evident that VLPs and their IC initiate SYK phosphorylation (Figure 1A). Western blot of the phosphorylated SYK showed similar results (Figure 1B; full-size image in Figure S4B). Quantitative analysis of Western blot data (Figure 1C) showed that both VLPs and IC cause a significant increase in SYK activation. However, none of the IC induced higher SYK phosphorylation level as compared with VLPs alone (Figure 1C).

One of the key markers of NLRP3 inflammasome activation is cytokine IL-1β. To validate our IC model, we used the specific NLRP3 inhibitor MCC950 in IL-1β secretion analysis. Results showed that inhibition of NLRP3 abrogates cytokine secretion (Figure 2D) and confirmed that inflammasome activation in our model is NLRP3-dependent. As our IC model consisting of VLPs and VLP-specific mAbs has been shown to activate the NLRP3 inflammasome, we induced NLRP3 inflammasome activation by IC to analyse SYK involvement [19]. First, we analysed NLRP3 receptor expression by Western blot (Figure 2A; full-size image in Figure S4A) and observed that reduced SYK phosphorylation was associated with decreased NLRP3 synthesis. Quantitative Western blot analysis of NLRP3 revealed that SYK inhibition causes a significant reduction of NLRP3 level in all microglia lysates treated with VLPs or any of the IC (Figure 2B). Another essential protein for the NLRP3 inflammasome assembly is adaptor protein ASC, which forms easily visible 1 µM speck-like structures [23]. We used immunocytochemical staining and observed cells under a fluorescent microscope to detect ASC specks. The results showed that both VLPs and their IC significantly increased ASC speck count per cell (Figure 2C–G). Additionally, SYK inhibition stopped ASC speck formation—the inhibitor reduced ASC speck count almost to control levels (Figure 2C).

To confirm SYK involvement in NLRP3 inflammasome activation, we also analysed changes in inflammatory cytokine secretion after SYK inhibition. The level of IL-1β secreted in cell growth medium was significantly reduced by the SYK inhibitor (Figure 2E). R406 reduced IL-1β concentration in all supernatants of microglia treated with either VLPs or their IC, except for IC formed by 11D2 mAbs (Figure 2E). Moreover, SYK inhibition caused a significant decrease in TNF-α secretion in both VLP- and IC-treated cells (Figure 2F). Together, these results demonstrate that both VLPs and their IC activate the NLRP3 inflammasome in a SYK-dependent manner. Additionally, given that VLPs are produced in yeast, we wanted to exclude a possible contribution of β-glucans in SYK activation. We used disassembled VLPs (VP1 pentamers) as a control prepared under the same conditions as the VLPs used in the experiments. We measured IL-1β secretion in the supernatants and pSYK expression in lysates of cells treated with disassembled VLPs (VP1 pentamers), zymosan, or ICs. The results revealed that disassembled VLPs (VP1 pentamers) do not induce IL-1β secretion or pSYK activation (Figures S1A and S3A), excluding the potential contribution of β-glucans from the VLP solution to SYK activation. This confirms that, in our model system, VLPs and their ICs are responsible for microglial response.

3.2 | The Role of SYK in Antigen Presentation and IC Phagocytosis

Further, we investigated whether SYK is involved in any functional properties of microglia, such as phagocytosis of VLPs and IC, and antigen presentation. We used pH-sensitive dye—pHrodo—to stain VLPs and then applied flow cytometry to analyse the uptake of stained VLPs and IC formed by stained VLPs and mAbs. Endocytosis inhibitor—cytochalasin D (Cyt D) was used as a negative control. As expected, VLPs and IC were effectively phagocytosed by microglia cells—a fluorescent signal was observed within the cells, and CytD diminished the pHrodo signal (Figure 3B,C). This proves that both VLPs and IC enter the cells through the phagocytosis mechanism.

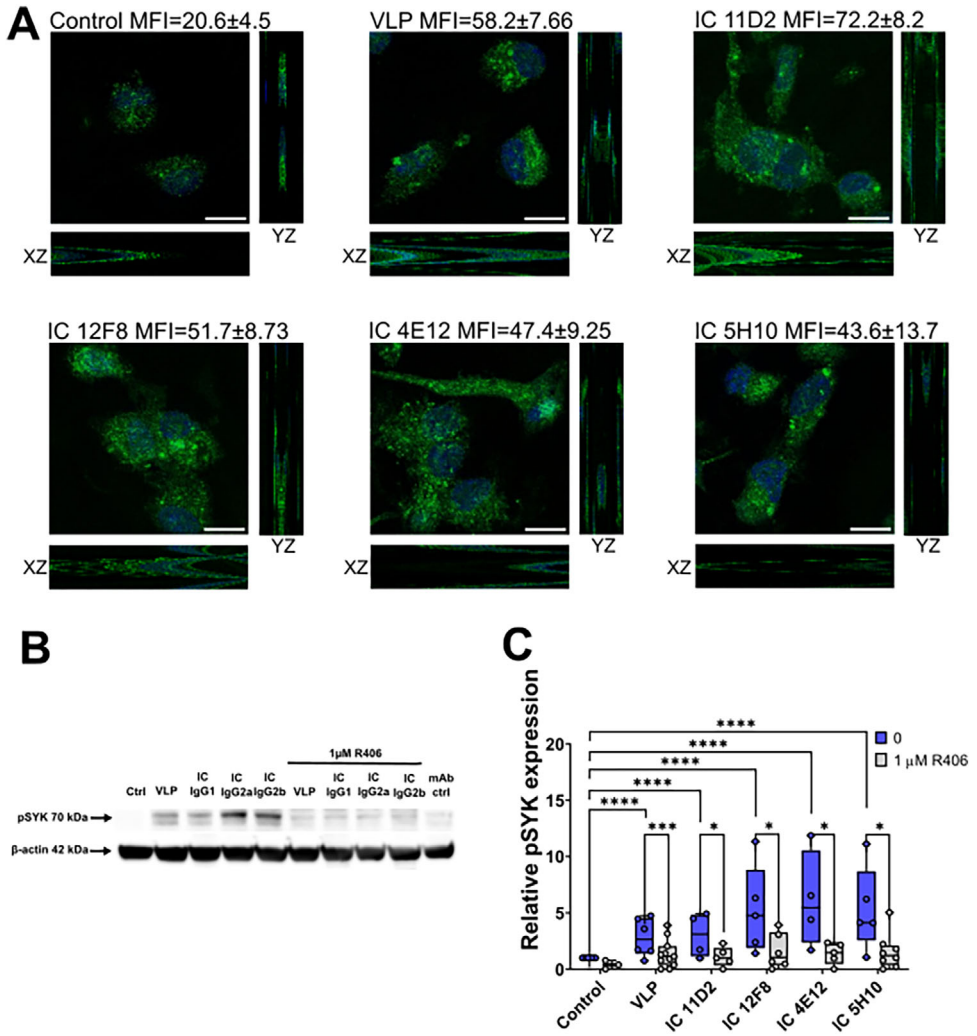

FIGURE 1 | SYK phosphorylation induced by VLPs and IC. Cells were treated with VLPs (20 μg/mL) and VLP-specific mAbs (7.5 μg/mL) for 24 h, and 1 μM of SYK inhibitor R406 was added 1 h before treatment. (A) Fluorescent microscopy images of stained pSYK (green) and nuclei with Hoechst33342 (blue), pSYK was stained with primary Ab anti-pSYK Y525/526 and secondary Ab-AlexaFluor 488. The experiment was repeated four times, and representative composite images and MFI ± SD per cell of 30 frames are shown. The scale bar is 10 μm. (B) Western blot data show the expression of the indicated protein in primary microglia lysates, with representative images of four to six independent experiments. (C) Quantification of pSYK expression from Western blot data normalised to a loading control, $N = 4–6$. Data are represented using a box plot with dots showing the number of individual experiments. Significance was established using one-way ANOVA followed by Tukey's test $^{*}p < 0.05$, $^{**}p < 0.01$, $^{***}p < 0.001$, $^{****}p < 0.0001$.

As the uptake of the VLPs and IC was confirmed, we examined whether the impact of SYK on macrophage activation was related to phagocytosis. The results showed that inhibition of SYK does not affect phagocytosis of VLPs or any of the IC (Figure 3D). Subsequently, we analysed the antigen presentation by measuring the major histocompatibility class II complex (MHC II) and CD86 molecule expression on the cell surface. MHC II presents peptide fragments derived from processed antigens to $CD4^+$ T cells, and CD86 is a costimulatory molecule that interacts with CD28 on $CD4^+$ T cells. Interaction between these markers and T cell receptors is necessary for an effective $CD4^+$ T cell response [24, 25]. We found that VLPs and all tested IC cause a significant increase in CD86 expression compared with the controls (Figure 3E). The MHC II expression levels were diverse, with different IC: its significant increase was observed when the IC was formed by mAb 11D2 (IgG1) and mAb 5H10 (IgG2b). Interestingly, both IC formed by IgG2a subclass mAbs (clones 12F8 and 4E12) did not induce MHC II expression, and its level was equal to the control level (Figure 3F). Furthermore, SYK inhibition significantly reduced CD86 and MHC II levels on the cell surface (Figure 3E,F). Consequently, these results indicate that antigen presentation depends on SYK signalling pathways, although SYK does not impact the phagocytosis of VLPs or their IC in microglia.

3.3 | Lipid Raft Formation in IC-Activated Microglia

Lipid rafts are highly organised membrane domains enriched with cholesterol/sphingolipids, which perform essential functions in immune cells as forming signalling platforms and participating in various types of endocytosis in the initial binding steps [26, 27]. Additionally, the signalling platforms formed of

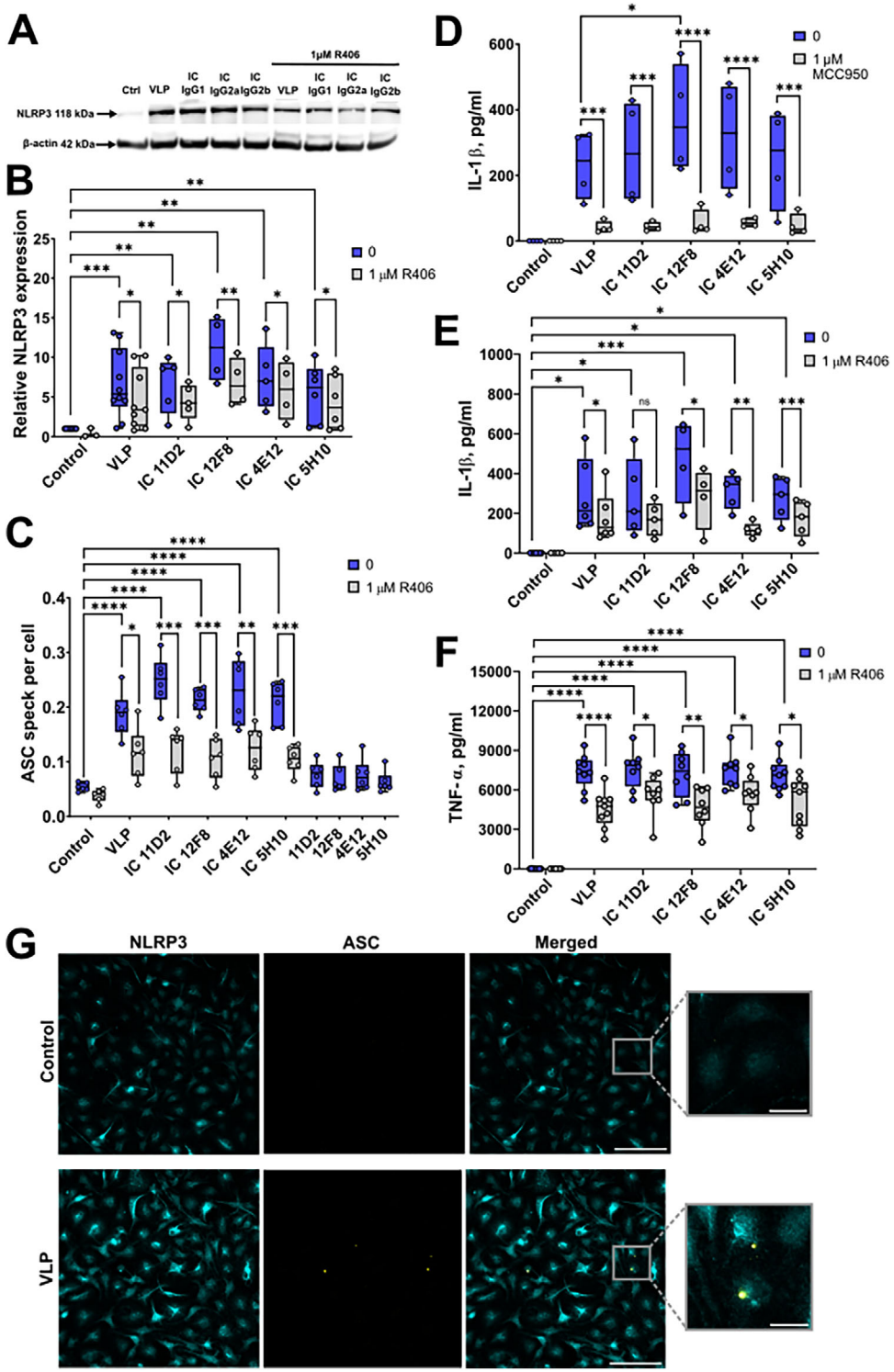

FIGURE 2 | The impact of SYK inhibition on NLRP3 activation. Cells were treated with VLPs (20 μg/mL) and mAbs (7.5 μg/mL) for 24 h, and 1 μM of SYK inhibitor R406 or NLRP3 inhibitor MCC950 was added 1 h before treatment. (A) Western blot data show the expression of the indicated protein in microglia lysates, and the images are representative of five to six experiments. (B) Quantification of NLRP3 expression from Western blot data, normalised to a loading control, $N = 5$–6. (C) Quantification of ASC speck formation in primary microglia, $N = 6$. (D, E) IL-1β secretion and (F) TNF-α secretion were tested by ELISA in microglia supernatants, (D) $N = 4$, (E) $N = 4$–6, (F) $N = 8$–9. (G) Fluorescent microscopy images of the immunostained NLRP3 (cyan) and ASC specks (yellow), NLRP3 was stained with primary Ab anti-NLRP and secondary Ab—AlexaFluor 488, ASC specks were stained with primary Ab anti-ASC-PE. Representative images are shown. The scale bars indicate 50 μm in large images and 20 μm in magnified images. In (B–F), data are represented using a box plot with dots showing the number of individual experiments. Significance was established using one-way ANOVA followed by Tukey's test *$p < 0.05$, **$p < 0.01$, ***$p < 0.001$, ****$p < 0.0001$.

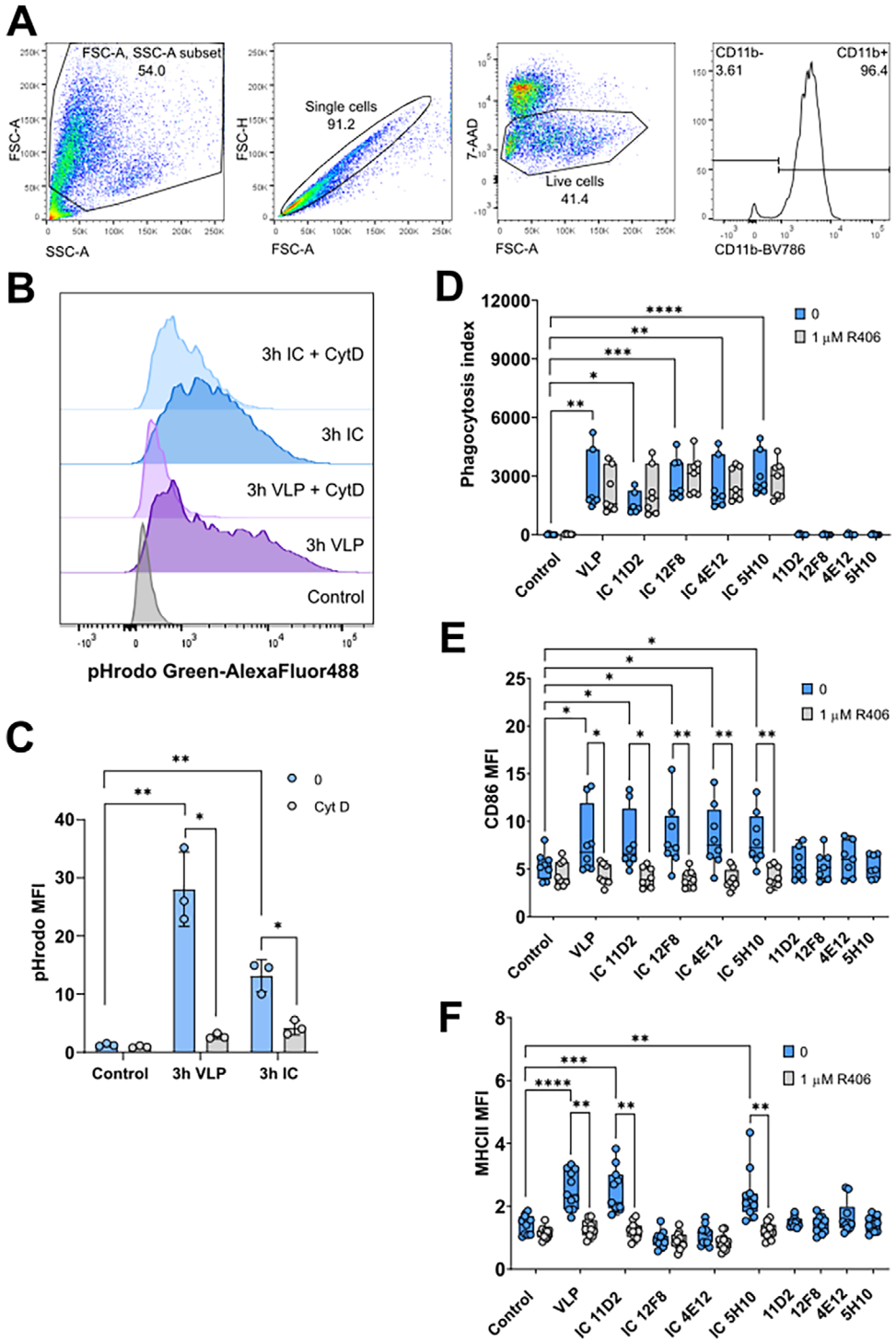

FIGURE 3 | The impact of SYK inhibition on phagocytosis and antigen presentation. Cells were treated with pHrodo-stained VLPs (10 μg/mL) and mAbs (7.5 μg/mL) for 3 h, 1 μM of SYK inhibitor R406 was added 1 h before treatment, and endocytosis inhibitor CytD was added for 30 min before treatment. pHrodo-stained VLP and IC phagocytosis, CD86, and MHC II expression were measured by flow cytometry. (A) The representative gating strategy is shown. (B) Representative histograms of phagocytosis inhibited by CytD. (C) pHrodo mean fluorescent intensity (MFI) values normalised to isotype control, $N = 3$. (D) Phagocytosis index of pHrodo particles: data are presented as mean fluorescent intensity multiplied by % of cells with phagocytosed pHrodo particles, $N = 7$. (E, F) CD86 and MHC II MFI values normalised to isotype control of each experiment, (E) $N = 8$, (F) $N = 11$. In (C), data are represented as a bar graph as mean ± SD with dots showing the number of individual experiments. Statistical significance was established using Student's *t*-test. In (D–F), data are represented using box plots with dots showing the number of individual experiments. Statistical significance was established using one-way ANOVA followed by Tukey's test *$p < 0.05$, **$p < 0.01$, ***$p < 0.001$, ****$p < 0.0001$.

lipid rafts concentrate the immunoreceptors and initiate various signalling pathways [28]. Consequently, we examined whether lipid rafts are also involved in the cellular uptake of IC. Cholera toxin subunit B (CTxB) with high affinity to the GM1 ganglioside was used as a stain for lipid rafts and plasma membrane, while IC-forming mAbs were also stained with anti-mouse IgG antibodies conjugated to AlexaFluor488. Microglia were analysed under the confocal microscope after immunocytochemical staining of lipid rafts and mAbs. In control wells, where cells were treated only with medium, there was little to no antibody signal, and more homogenous membrane staining with CtxB was observed, contrary to IC-activated cells, which displayed distinct clusters stained with CTxB and mAbs (Figure 4A). The colocalisation analysis of IC and CtxB lipid raft staining suggests that microglia form lipid raft-like structures upon activation by IC (Figure 4B). We also analysed raft formation under the wide-field microscope to visualize the overall distribution and clustering of lipid rafts in microglia. Wide-field imaging revealed that IC-treated cells show more clustered CtxB staining, which complies with the stained mAbs signal and significantly increased fluorescence intensity (Figure 4C,D). These results suggest that lipid rafts are involved in immune signalling induced by viral IC. Finally, to clarify the relationship between SYK and lipid raft formation, SYK inhibitor conditions were applied. The results showed that lipid raft clustering is independent of SYK activity, as raft formation did not change in the presence of the inhibitor (Figure S2). Therefore, lipid raft clustering occurs upstream of SYK activation.

4 | Discussion

Our study focused on macrophage activation by VLPs and their IC and the processes involved in inflammasome activation. We used the IC model, composed of viral proteins and their specific mAbs of different IgG subtypes that resemble naturally occurring IC, while more extensively used IC models are albumin conjugated to IgG and streptavidin conjugated to IgG [29]. Our cell model was microglia, which, compared with monocytes or monocyte-derived macrophages, also encounter IC. Microglia represent a relevant model for analysing tissue-resident macrophage response, as microglia have the same defence mechanisms, a high activation threshold, and a longer lifetime [30, 31]. Consequently, we observed that both VLPs and their IC cause an inflammatory response in microglia and activate the NLRP3 inflammasome. In this study, NLRP3-dependent IL-1β secretion in the presence of IC was determined using the specific NLRP3 inhibitor MCC950, which significantly reduced cytokine secretion. These findings coincide with previous results [19]. Besides, we recorded elevated phagocytosis, which might act as a contributor to the second signal for NLRP3 inflammasome activation.

FcγRs are broadly expressed on the surface of myeloid cells, including microglia. The presence of opsonised pathogenic triggers induces FcγRs crosslinking and downstream immune signalling. The receptor engagement leads to activation of Src family kinases and phosphorylation of ITAM, which activates SYK, leading to phosphorylation of its downstream substrates such as phosphoinositide 3-kinase, extracellular regulated kinase, protein kinase C-δ, or phospholipase Cγ [32, 33]. One of the final effects of SYK downstream signalling is NF-kB factor activation. The substrates of SYK phosphorylation, such as phospholipase Cγ or protein kinase C-δ, transfer a signal downstream to CARD9, which induces NF-kB activation [33, 34]. This mechanism is usually related to pathogen-induced inflammatory response and explains SYK involvement in NLRP3 activation. However, whether this mechanism would apply to IC-induced inflammation in myeloid cells is unclear. Therefore, we aimed to investigate SYK involvement in the pathway of inflammasome activation by IC. We found that phosphorylation of SYK is important in NLRP3 activation by IC. Moreover, we observed that inhibition of SYK reduces NLRP3 synthesis, ASC speck formation, and IL-1β secretion, all the major markers of the inflammasome activation. Previously, using small interfering siRNA to silence NLRP3, we showed that the increase in IL-1β mediated by VLPs and IC indeed depends on the NLRP3 [19]. Therefore, reduced IL-1β secretion and ASC speck formation after inhibition of SYK reveal that SYK plays a significant role in NLRP3 activation by viral IC. Furthermore, we showed that the inhibition of SYK significantly affects TNF-α secretion. NLRP3 inflammasome activation is typically described as a two-step process: priming and activation. Priming usually involves NF-κB signalling downstream of Toll-like receptors or other signals that lead to increased protein synthesis of NLRP3 and pro-IL-1β. Then the NLRP3 inflammasome can be activated by a wide range of triggers, such as PAMPs and DAMPs [6, 35]. NF-κB is a key transcription factor for genes regulating TNF-α cytokine secretion, which in turn may activate NF-κB [36]. Therefore, a reduction in TNF-α secretion combines SYK activation and NF-κB activity. This suggests that after activation by IC, SYK activates NF-κB, which then initiates NLRP3 expression, leading to NLRP3 inflammasome activation and IL-1β secretion. However, SYK inhibition does not entirely block NLRP3 activation. Persistent NLRP3 expression suggests SYK-independent priming pathways in NLRP3 activation, as other signal transduction pathways may activate NF-κB and the NLRP3 inflammasome. For instance, earlier we showed that VLPs activate the NLRP3 inflammasome via lysosomal rupture and the release of cathepsins [37]. This aligns with other literature describing processes in which activators (cholesterol crystals, nanoparticles) trigger an interplay with pathways, such as lysosomal damage, oxidative stress, that assemble to NLRP3 activation [38, 39].

Macrophages contribute to immune response via NLRP3 inflammasome activation and act as antigen-presenting cells to $CD4^+$ T cells [40]. MHC II molecule presents antigens degraded in phagolysosomes to $CD4^+$ T cells. However, efficient T cell activation requires not only the direct contact with the antigen peptide in the MHC II complex but also the involvement of CD28 [41]. Absence of this costimulatory signal leads to T cell anergy [42]. CD86 is one of the costimulatory molecules constitutively expressed by antigen-presenting cells (APCs), which is thus important in the early interactions of T cells and APCs [42]. The FcγRs are key regulators in antigen presentation, and SYK plays an essential role in the signalling cascade initiated by FcRs [14, 43]. However, there is insufficient data on the impact of different IC on antigen presentation in macrophages and the involvement of SYK in this process. Thus, we analysed SYK's involvement in the expression of molecules related to antigen presentation on microglia cells treated with different IC formed by VLPs and IgG of different subtypes. We showed that both VLPs and their

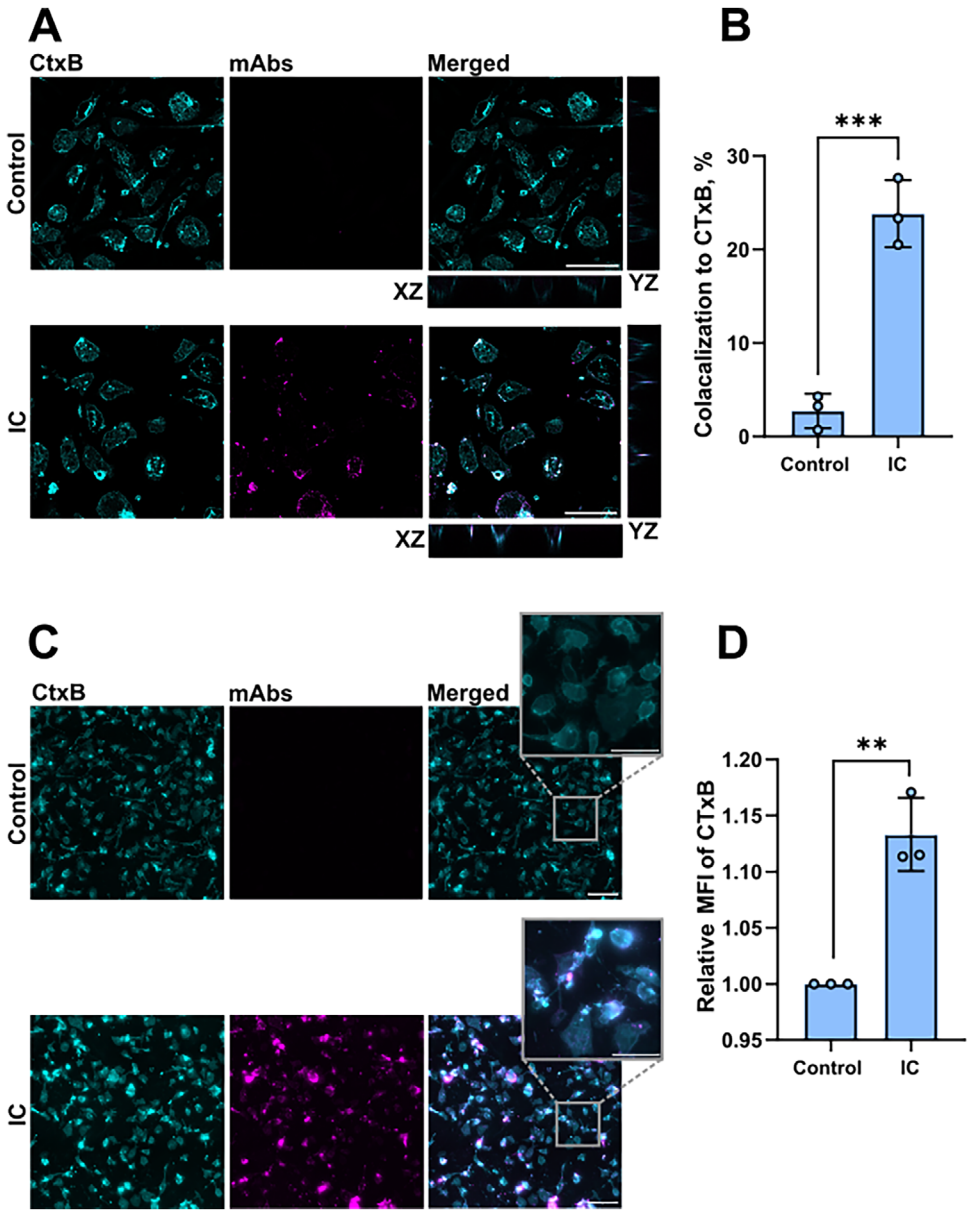

FIGURE 4 | Visualisation of lipid rafts and IC interaction on the cell surface. Cells were treated with VLPs (20 μg/mL) and mAbs (7.5 μg/mL) for 3 h. Lipid rafts were stained with CTxB-AF594 (cyan) 30 min before fixation. IC on fixed cells were stained with secondary Ab-AF488 (magenta). (A) Representative fluorescent microscopy images of lipid rafts and IC taken with the LEICA Sp8 confocal microscope. Representative composite images of 32 steps are shown. The scale bar is 50 μm. (B) Quantified colocalisation to CTxB shows the fraction of CTxB signal overlapping with IC signal. Mander's overlap coefficient was calculated with the ImageJ Fiji BIOP JACoP plugin, $N = 3$. (C) Representative fluorescent microscopy images of lipid rafts and IC taken with a Nikon Eclipse Ti-2E wide-field microscope. The scale bars are 100 μm in the large images and 50 μm in the magnified images. (D) Relative MFI of CTxB signal per picture was calculated with NIS-elements and normalised to controls, $N = 3$. (A, C) The experiments were repeated at least three times, and representative images are shown. In (B, D), data are presented using a bar graph as mean ± SD with dots showing the number of individual experiments. Statistical significance was established using Student's *t*-test, $^{**}p < 0.01$, $^{***}p < 0.001$.

IC induce antigen presentation in microglia, as the expression of CD86 and MHC II molecules significantly increases upon treatment with VLPs and IC formed by VLP-specific mAbs of IgG1 and IgG2b subclasses. Although IgG2a is mainly related to proinflammatory signalling compared with other IgG molecules in mice, and IC formed by IgG2a mAbs (clones 12F8 and 4E12) induced higher CD86 expression on the surface of microglia, these IC did not affect MHC II expression. Previously, we have shown that the same IgG2a mAbs have the highest affinity to the VLPs, form complexes of relatively bigger size, and enhance inflammation in microglia [12, 19]. Thus, the properties of the IC may influence antigen presentation in APCs. Moreover, we showed that SYK also influences the antigen presentation, as the inhibition of SYK reduced MHC II and CD86 expression to control levels. Usually, costimulatory molecule expression is upregulated through PRR-mediated signalling, and MHC II expression is related to NF-κB activation [44, 45]. This may suggest that SYK blocking interferes with signal transduction downstream to NF-κB and causes a reduced MHC II and CD86 expression.

Further, we analysed lipid raft formation in IC-activated microglia and the involvement of SYK in this process. Lipid rafts are dynamic plasma membrane microdomains rich in cholesterol, sphingolipids, and proteins [46]. They are critical for cellular processes, especially for immune cells, as they participate in endocytosis, immune signalling, compartmentalisation, and host–pathogen interaction [47, 48]. Most immune cells have their receptors localised in lipid rafts, as they can concentrate signalling molecules and create signalling platforms [48, 49]. Lipid raft signalling platforms are also enriched in SRC kinases, which operate upstream of SYK in signal transduction pathways [10, 28]. Additionally, antigen capture and endocytosis often occur at lipid raft domains, as rafts contain many receptors of pathogens and vesicle-forming proteins [28, 50]. When analysing microglia activation by IC formed by VLPs and VLP-specific mAbs, we observed lipid raft colocalisation with IC. This suggests that IC activates macrophages through a lipid raft signalling platform where SYK and other signal transduction molecules are located. Upon SYK activation, the signal is transferred to NF-κB, leading to gene expression of NLRP3, IL-1β, and TNF-α that initiate the inflammatory response.

Summarising, we showed that after being phagocytosed through lipid rafts, IC activate primary microglia and cause NLRP3 inflammasome activation, including NLRP3 expression, ASC speck formation, and cytokine secretion dependent on SYK signalling. SYK is also involved in the ability of microglia to present antigens via up-regulation of MHC II and CD86 molecule expression. Interestingly, IC formed by IgG2a subclass antibody did not affect MHC II exposure on the cell surface, contrary to IC formed by IgG1 and IgG2b antibodies that significantly increased MHC II expression. Our previous studies and the current data show that characteristics of IC-forming antibody can shape the effector functions of macrophages, demonstrating the role of a particular IgG subclass in FcγR activation. Together, these findings give insights into IC-mediated inflammatory responses induced by viral antigens and their specific antibodies consequently to viral infections, vaccination, or antibody-based therapies.

Author Contributions

K.M. performed the experiments, analysed the data, and wrote the manuscript. A.L. was responsible for the idea, and together with K.M. designed the experiments. M.N. was responsible for VLPs preparation and characterisation. A.L. and A.Ž. were responsible for the final manuscript revision.

Acknowledgements

This research was partially funded by the Science Promotion Fund of Vilnius University, a grant for young scientists awarded to Dr. A. Lučiūnaitė.

Ethics Statement

The manuscript does not contain experiments using human studies. All experiments involving mice were conducted in accordance with institutional guidelines and received approval from the local ethics committee. Only the organs of C57BL/6 mice were used for primary cell culture preparation. Mice were grown at Life Sciences Center of Vilnius University (Vilnius, Lithuania), which has State Food and Veterinary Service permissions to breed and use experimental animals for scientific purposes (Veterinary certificate No. LT 59–13-001 and Permission No. LT 61-13-004).

Conflicts of Interest

The authors declare no conflicts of interest.

Data Availability Statement

All data used to support the findings of this study are included within the article. The data that support the findings of this study are available from the corresponding author upon reasonable request.

Data Limitation and Perspectives

Despite the significance and novelty of our findings, we acknowledge several limitations of our study. Firstly, the study would have benefited from the inclusion of additional cell populations phagocytosing IC, such as professional APC beyond macrophages, to provide a more comprehensive analysis of the inflammatory response. Additionally, our study was limited by the mouse-derived mAbs specific to VLPs, which restricted us to using primary mouse culture as a cell model. Although primary murine cells offer valuable insights, they do not replicate the complexity of human cells, which limits the translatability of the study. Lastly, our use of mAbs to form IC allowed us to examine the impact of specific antibody properties on the inflammatory response; however, IC composed of mAbs does not represent the heterogeneity of natural IC.

Peer Review

For transparency, the peer review documents associated with this article are available at https://doi.org/10.1002/eji.70199.

References

1. M. D. Park, A. Silvin, F. Ginhoux, and M. Merad, "Macrophages in Health and Disease," *Cell* (2022): 4259–4279, https://doi.org/10.1016/j.cell.2022.10.007, PubMed PMID: 36368305.

2. T. Gong, L. Liu, W. Jiang, and R. Zhou, "DAMP-Sensing Receptors in Sterile Inflammation and Inflammatory Diseases," *Nature Reviews Immunology* (2020): 95–112, https://doi.org/10.1038/s41577-019-0215-7, Nature Research, PubMed PMID: 31558839.

3. N. Kelley, D. Jeltema, Y. Duan, and Y. He, "The NLRP3 Inflammasome: An Overview of Mechanisms of Activation and Regulation," *International Journal of Molecular Sciences MDPI AG;* (2019), https://doi.org/10.3390/ijms20133328, PubMed PMID: 31284572.

4. A. Baroja-Mazo, F. Martín-Sánchez, A. I. Gomez, et al., "The NLRP3 Inflammasome Is Released as a Particulate Danger Signal That Amplifies the Inflammatory Response," *Nature Immunology* 15, no. 8 (2014): 738–748, https://doi.org/10.1038/ni.2919, PubMed PMID: 24952504.

5. F. G. Bauernfeind, G. Horvath, A. Stutz, et al., "Cutting Edge: NF-κB Activating Pattern Recognition and Cytokine Receptors License NLRP3 Inflammasome Activation by Regulating NLRP3 Expression," *The Journal of Immunology* 183, no. 2 (2009 Jul 15): 787–791, https://doi.org/10.4049/jimmunol.0901363, PubMed PMID: 19570822.

6. S. Feng, M. C. Wierzbowski, K. Hrovat-Schaale, et al., "Mechanisms of NLRP3 Activation and Inhibition Elucidated by Functional Analysis of Disease-Associated Variants," *Nature Immunology* 26, no. 3 (2025 Mar 1): 511–523, https://doi.org/10.1038/s41590-025-02088-9, PubMed PMID: 39930093.

7. R. M. McManus, M. P. Komes, and A. Griep, "NLRP3-Mediated Glutaminolysis Controls Microglial Phagocytosis to Promote Alzheimer's Disease Progression," *Immunity* 58, no. 2 (2025 Feb 11): 326–343.e11, https://doi.org/10.1016/j.immuni.2025.01.007, PubMed PMID: 39904338.

8. E. Sefik, R. Qu, C. Junqueira, et al., "Inflammasome Activation in Infected Macrophages Drives COVID-19 Pathology," *Nature* 606, no.

7914 (2022 Jun 16): 585–593, https://doi.org/10.1038/s41586-022-04802-1, PubMed PMID: 35483404.

9. O. Gross, H. Poeck, M. Bscheider, et al., "Syk Kinase Signalling Couples to the Nlrp3 Inflammasome for Anti-Fungal Host Defence," *Nature* 459, no. 7245 (2009 May 21): 433–436, https://doi.org/10.1038/nature07965, PubMed PMID: 19339971.

10. Y. Tohyama and H. Yamamura, "Protein Tyrosine Kinase, Syk: A Key Player in Phagocytic Cells," *Journal of Biochemistry* (2009): 267–273, https://doi.org/10.1093/jb/mvp001, PubMed PMID: 19124456.

11. Y. C. Lin, D. Y. Huang, J. S. Wang, et al., "Syk Is Involved in NLRP3 Inflammasome-Mediated Caspase-1 Activation Through Adaptor ASC Phosphorylation and Enhanced Oligomerization," *Journal of Leukocyte Biology* 97, no. 5 (2015 May 1): 825–835.

12. F. Nimmerjahn and J. V. Ravetch, "Fcγ Receptors as Regulators of Immune Responses," *Nature Reviews Immunology* (2008): 34–47, https://doi.org/10.1038/nri2206, PubMed PMID: 18064051.

13. S. Bournazos, A. Gupta, and J. V. Ravetch, "The Role of IgG Fc Receptors in Antibody-Dependent Enhancement," *Nature Reviews Immunology* (2020): 633–643, https://doi.org/10.1038/s41577-020-00410-0, Nature Research, PubMed PMID: 32782358.

14. F. Junker, J. Gordon, and O. Qureshi, "Fc Gamma Receptors and Their Role in Antigen Uptake, Presentation, and T Cell Activation," *Frontiers in Immunology Frontiers Media SA* (2020), https://doi.org/10.3389/fimmu.2020.01393, PubMed PMID: 32719679.

15. M. Guilliams, P. Bruhns, Y. Saeys, H. Hammad, and B. N. Lambrecht, "The Function of Fcγ Receptors in Dendritic Cells and Macrophages," *Nature Reviews Immunology* (2014): 94–108, https://doi.org/10.1038/nri3582, PubMed PMID: 24445665.

16. W. Hoepel, H. J. Chen, C. E. Geyer, et al., "High Titers and Low Fucosylation of Early human Anti-SARS-CoV-2 IgG Promote Inflammation by Alveolar Macrophages," *Science Translational Medicine* 13, no. 596 (2021 Jun 2), https://doi.org/10.1126/scitranslmed.abf8654, PubMed PMID: 33979301.

17. C. Junqueira, Â. Crespo, S. Ranjbar, et al., "FcγR-mediated SARS-CoV-2 Infection of Monocytes Activates Inflammation," *Nature* 606, no. 7914 (2022 Jun 16): 576–584, https://doi.org/10.1038/s41586-022-04702-4, PubMed PMID: 35385861.

18. A. Grebe, F. Hoss, and E. Latz, "NLRP3 inflammasome and the IL-1 Pathway in Atherosclerosis. Circulation Research," *Lippincott Williams and Wilkins* (2018): 1722–1740, PubMed PMID: 29880500., https://doi.org/10.1161/CIRCRESAHA.118.311362.

19. A. Lučiūnaitė, K. Mašalaitė, I. Plikusiene, et al., "Structural Properties of Immune Complexes Formed by Viral Antigens and Specific Antibodies Shape the Inflammatory Response of Macrophages," *Cell Bioscience* 14, no. 1 (2024 Dec 1), https://doi.org/10.1186/s13578-024-01237-1.

20. M. Norkiene, J. Stonyte, D. Ziogiene, E. Mazeike, K. Sasnauskas, and A. Gedvilaite, "Production of Recombinant VP1-Derived Virus-Like Particles From Novel Human Polyomaviruses in Yeast," *BMC Biotechnology [Electronic Resource]* 15, no. 1 (2015 Aug 4), https://doi.org/10.1186/s12896-015-0187-z, PubMed PMID: 26239840.

21. P. S. Shen, D. Enderlein, C. D. S. Nelson, et al., "The Structure of Avian Polyomavirus Reveals Variably Sized Capsids, Non-Conserved Inter-Capsomere Interactions, and a Possible Location of the Minor Capsid Protein VP4," *Virology* 411, no. 1 (2011 Mar 1): 142–152, https://doi.org/10.1016/j.virol.2010.12.005, PubMed PMID: 21239031.

22. M. Prinz, T. L. Tay, Y. Wolf, and J. S. Microglia, "Unique and Common Features With Other Tissue Macrophages," *Acta Neuropathologica* (2014): 319–331, https://doi.org/10.1007/s00401-014-1267-1, PubMed PMID: 24652058.

23. A. Nagar, R. Bharadwaj, M. O. F. Shaikh, and A. Roy, "What Are NLRP3-ASC Specks? An Experimental Progress of 22 Years of Inflammasome Research," *Frontiers in Immunology Frontiers Media SA;* (2023), https://doi.org/10.3389/fimmu.2023.1188864, PubMed PMID: 37564644.

24. A. Mangalam, M. Rodriguez, and C. David, "Role of MHC Class II Expressing CD4+ T Cells in Proteolipid protein91-110-Induced EAE in HLA-DR3 Transgenic Mice," *European Journal of Immunology* 36, no. 12 (2006 Dec): 3356–3370, https://doi.org/10.1002/eji.200636217, PubMed PMID: 17125142.

25. N. Halliday, C. Williams, A. Kennedy, et al., "CD86 Is a Selective CD28 Ligand Supporting FoxP3+ Regulatory T Cell Homeostasis in the Presence of High Levels of CTLA-4," *Frontiers in immunology* 11 (2020 Dec 8), PubMed PMID: 33363541, https://doi.org/10.3389/fimmu.2020.600000.

26. B. J. Nichols, "GM1-Containing Lipid Rafts Are Depleted within Clathrin-Coated Pits," *Current Biology* 13 (2003): 686–690, https://doi.org/10.1016/s0960-9822(03)00209-4.

27. N. M. Hooper and J. V. Rushworth, "Lipid Rafts: Linking Alzheimer's Amyloid-β Production, Aggregation, and Toxicity at Neuronal Membranes," *International Journal of Alzheimer's Disease* (2011), https://doi.org/10.4061/2011/603052.

28. E. Sezgin, I. Levental, S. Mayor, and C. Eggeling, "The Mystery of Membrane Organization: Composition, Regulation and Roles of Lipid Rafts," *Nature Reviews Molecular Cell Biology* (2017): 361–374, https://doi.org/10.1038/nrm.2017.16, PubMed PMID: 28356571.

29. A. Deb, K. Lott, A. Miceli, and B. L. F. Kaplan, "Optimization of IgG1 Immune Complexes to Stimulate Cytokine Production in Innate Cells," *Journal of Immunological Methods* (2025 Apr 1): 539, PubMed PMID: 40081523, https://doi.org/10.1016/j.jim.2025.113851.

30. A. M. Jurga, M. Paleczna, and K. Z. Kuter, "Overview of General and Discriminating Markers of Differential Microglia Phenotypes," *Frontiers in Cellular Neuroscience* 14 (2020 Aug 6), https://doi.org/10.3389/fncel.2020.00198.

31. S. A. Amici, J. Dong, and M. Guerau-de-Arellano, "Molecular Mechanisms Modulating the Phenotype of Macrophages and Microglia," *Frontiers in Immunology Frontiers Media SA* (2017), https://doi.org/10.3389/fimmu.2017.01520.

32. C. A. Lowell, "Src-Family and Syk Kinases in Activating and Inhibitory Pathways in Innate Immune Cells: Signaling Cross Talk," *Cold Spring Harbor Perspectives in Biology* (2011): 1–16, PubMed PMID: 21068150, https://doi.org/10.1101/cshperspect.a002352.

33. D. Strasser, K. Neumann, H. Bergmann, et al., "Syk Kinase-Coupled C-Type Lectin Receptors Engage Protein Kinase C-δ to Elicit Card9 Adaptor-Mediated Innate Immunity," *Immunity* 36, no. 1 (2012 Jan 27): 32–42, https://doi.org/10.1016/j.immuni.2011.11.015, PubMed PMID: 22265677.

34. W. J. Pandori, T. S. Lima, S. Mallya, T. H. Kao, L. Gov, and M. B. Lodoen, "*Toxoplasma gondii* Activates a Syk-CARD9-NF-κB Signaling Axis and Gasdermin Dindependent Release of IL-1β During Infection of Primary human Monocytes," *Plos Pathogens* 15, no. 8 (2019), https://doi.org/10.1371/journal.ppat.1007923, PubMed PMID: 31449558.

35. S. G. Boaru, E. Borkham-Kamphorst, E. Van De Leur, E. Lehnen, C. Liedtke, and R. Weiskirchen, "NLRP3 Inflammasome Expression Is Driven by NF-κB in Cultured Hepatocytes," *Biochemical and Biophysical Research Communications* 458, no. 3 (2015 Mar 13): 700–706, https://doi.org/10.1016/j.bbrc.2015.02.029, PubMed PMID: 25686493.

36. T. Liu, L. Zhang, D. Joo, and S. C. Sun, "NF-κB Signaling in Inflammation," *Signal Transduction and Targeted Therapy* PubMed PMID: 29158945 (2017), https://doi.org/10.1038/sigtrans.2017.23.

37. A. Lučiūnaitė, I. Dalgėdienė, R. Žilionis, et al., "Activation of NLRP3 Inflammasome by Virus-Like Particles of Human Polyomaviruses in Macrophages," *Frontiers in immunology* 13 (2022 Mar 9), PubMed PMID: 35355981, https://doi.org/10.3389/fimmu.2022.831815.

38. M. Yalcinkaya and A. R. Tall, "Cholesterol Crystals as Triggers of NLRP3 Inflammasome Activation in Atherosclerosis," *Current Atherosclerosis Reports* (2025), https://doi.org/10.1007/s11883-025-01323-w, PubMed PMID: 40748587.

39. R. J. Vandebriel, S. Remy, J. P. Vermeulen, et al., "Pathways Related to NLRP3 Inflammasome Activation Induced by Gold Nanorods," *Inter-*

national Journal of Molecular Sciences 23, no. 10 (2022 May 1), https://doi.org/10.3390/ijms23105763.

40. C. E. Arnold, P. Gordon, R. N. Barker, and H. M. Wilson, "The Activation Status of human Macrophages Presenting Antigen Determines the Efficiency of Th17 Responses," *Immunobiology* 220, no. 1 (2015 Jan 1): 10–19, https://doi.org/10.1016/j.imbio.2014.09.022, PubMed PMID: 25454489.

41. C. C. Tung, A. P. S. Rathore, and A. L. St John, "Conventional and Non-Conventional Antigen Presentation by Mast Cells," *Discovery Immunology* (2023), https://doi.org/10.1093/discim/kyad016.

42. M. G. Agadjanyan, J. J. Kim, N. Trivedi, et al. CD86 (B7-2) Can Function to Drive MHC-Restricted Antigen-Specific CTL Responses in Vivo1 [Internet]. 1999, https://academic.oup.com/jimmunol/article/162/6/3417/8041711.

43. K. Nakashima, T. Kokubo, M. Shichijo, Y. F. Li, T. Yura, and N. Yamamoto, "A Novel Syk Kinase-Selective Inhibitor Blocks Antigen Presentation of Immune Complexes in Dendritic Cells," *European Journal of Pharmacology* 505, no. 1–3 (2004 Nov 28): 223–228, https://doi.org/10.1016/J.EJPHAR.2004.10.024, PubMed PMID: 15556156.

44. S. L. Swain, K. K. McKinstry, and T. M. Strutt, "Expanding Roles for CD4 + T Cells in Immunity to Viruses," *Nature Reviews Immunology* (2012): 136–148, https://doi.org/10.1038/nri3152, PubMed PMID: 22266691.

45. D. T. T. Hang, J. Y. Song, M. Y. Kim, J. W. Park, and Y. K. Shin, "Involvement of NF-κB in Changes of IFN-γ-Induced CIITA/MHC-II and iNOS Expression by Influenza Virus in Macrophages," *Molecular Immunology* 48, no. 9–10 (2011 May): 1253–1262, https://doi.org/10.1016/j.molimm.2011.03.010, PubMed PMID: 21481937.

46. M. Goldmann, F. Schmidt, Z. Cseresnyés, et al., "The Lipid Raft-Associated Protein Stomatin Is Required for Accumulation of Dectin-1 in the Phagosomal Membrane and for Full Activity of Macrophages Against *Aspergillus fumigatus*," *mSphere* 8, no. 1 (2023 Feb 21), https://doi.org/10.1128/msphere.00523-22, PubMed PMID: 36719247.

47. Y. I. Miller, J. M. Navia-Pelaez, M. Corr, and T. L. Yaksh, "Lipid Rafts in Glial Cells: Role in Neuroinflammation and Pain Processing," *Journal of Lipid Research American Society for Biochemistry and Molecular Biology Inc* (2020): 655–666, https://doi.org/10.1194/jlr.TR119000468, PubMed PMID: 31862695.

48. R. Kulkarni, E. A. C. Wiemer, and W. Chang, "Role of Lipid Rafts in Pathogen-Host Interaction—A Mini Review," *Frontiers in Immunology Frontiers Media SA* (2022), https://doi.org/10.3389/fimmu.2021.815020, PubMed PMID: 35126371.

49. J. M. Ruysschaert and C. Lonez, "Role of Lipid Microdomains in TLR-Mediated Signalling," *Biochimica et Biophysica Acta—Biomembranes* (2015): 1860–1867, https://doi.org/10.1016/j.bbamem.2015.03.014, PubMed PMID: 25797518.

50. K. Sapon, R. Manka, T. Janas, and T. Janas, "The Role of Lipid Rafts in Vesicle Formation," *Journal of Cell Science Company of Biologists Ltd;* (2023), https://doi.org/10.1242/jcs.260887, PubMed PMID: 37158681.

Supporting Information

Additional supporting information can be found online in the Supporting Information section.

Supporting File: eji70199-sup-0001-SuppMat.pdf.